Controllable Synthesis of $Bi_2Fe_4O_9$ Nanocrystal with High Active Facets and the Enhanced Visible Light Photoelectrochemical Property

Yan ZHANG[1, 2, a*], Yanhua PENG[2], Jinqiu ZHANG[2], Chunhu LI[1] , and Jianqiang YU[2,3,b]

[1] College of Chemistry and Chemical Engineering, Ocean University of China, Qingdao 266045, China;
[2] Faculty of Chemical Science and Engineering, Qingdao University, Qingdao, 266071, China;
[3] Laboratory of Clean Energy Chemistry and Materials, Lanzhou Institute of Chemical Physics, Chinese Academy of Science, Lanzhou, 730000, China
[a]zhangyanchem@qdu.edu.cn, [b]yjq@licp.cas.cn

Abstract. $Bi_2Fe_4O_9$ nanocrystals with high active facets were controllably synthesized via a chemical co-precipitation process followed by a hydrothermal treatment at various microenvironment. The nanocrystals can be controlled preferentially to grow along (001) and show flat side facets of (110) and ($\bar{1}$10). The photoinduced charge-transfer property of $Bi_2Fe_4O_9$ was significantly improved. Such a high photo-to-current conversion efficiency is ascribed to the synergistic effect of energy band structure and the high reactivity of exposed (110) and ($\bar{1}$10) facets. The high surface energy at the interface of the $Bi_2Fe_4O_9$ efficiently reduced the recombination of photoinduced electron-hole pairs, and thus increasing the lifetime of charge carriers and enhancing the photo-to-current efficiency of the $Bi_2Fe_4O_9$.
Keywords: Photoelectrochemical; Water splitting; Bismuth Vanadate; Solar Energy; Visible-light

1 Introduction

Photoelectrochemical water splitting has attracted increasing interest over the past decades, because it is a very promising technology for converting solar energy into chemical energy and for developing environment technology. However, UV-light active photocatalytic inorganic nanomaterials, such as titania, can only be activated by wavelengths in the near-UV region (< 400 nm) and cannot efficiently utilize the major part of sunlight to photoelectrochemical water splitting. Therefore, the development of the visible-light-driven photocatalysts for water splitting seems to be a promising way from the viewpoint of using solar energy.

As one of the most important ferrite binary oxides with the orthorhombic structure, bismuth ferrioic is usually used as a ferromagnetic material with magnetic properties

* Corresponding author: zhangyanchem@qdu.edu.cn

strongly dependent on the state of chemical order. However, it has recently gained importance as a material for electronic, field-emission, electrochemical, sensors, and lithium ion battery devices [1-3]. As a typical bismuth ferrite, orthorhombic $Bi_2Fe_4O_9$ is an interesting material for photocatalytic and photoelectrochemical applications. It has been reported that both $Bi_2Fe_4O_9$ nanosheets (25–35 nm thick) and nanoplates (80–100 nm thick) exhibit high visible-light photocatalytic activity [4, 5].

However, research works on the intrinsic properties and applications of $Bi_2Fe_4O_9$ are still hindered greatly by the difficulty in the controllable synthesis of $Bi_2Fe_4O_9$ nanocrystal with high active facets, because the kinetics of phase formation in the Bi_2O_3–Fe_2O_3 system can easily lead to the coexistence of compounds such as $BiFeO_3$, $Bi_2Fe_4O_9$ and $Bi_{25}FeO_{40}$. [6] However, problems such as harsh reaction conditions, utilization of volatile organic solvents, high temperature, large dimensions, poor yields of the desired products still exist in these methods. It is still a challenge to control the synthesis of pure-phase $Bi_2Fe_4O_9$ nanocrystals. Recently we have synthesized single-phase $Bi_2Fe_4O_9$ nanocrystals through a facile chemical co-precipitation process and observed prompt, steady and significant photocurrent in the thin-film photoelectrodemade of $Bi_2Fe_4O_9$ nanocrystals under visible-light irradiation, suggesting that $Bi_2Fe_4O_9$ is a promising material for photoelectrode and solar energy conversion applications.

In this paper, $Bi_2Fe_4O_9$ nanocrystals have been controllably synthesized via a chemical co-precipitation process followed by a hydrothermal synthesis through tuning the synthesis microenvironment. They exhibit high performance of photo-to-current conversion under visible-light.

2 Experimental Section

2.1 Synthesis

$Bi_2Fe_4O_9$ nanocrystals were prepared via a chemical co-precipitation process. Firstly, 3 mmol of $Bi(NO_3)_3{\cdot}5H_2O$ and 6 mmol of $Fe(NO_3)_3{\cdot}9H_2O$ were dissolved into 3 mL of HNO_3 (2 M) at room temperature. After complete dissolution, the mix solutions were titrated by dropwise addition of ammonia solution (SinoChem Chemical, 28-30% NH_3) under stirring, brown precipitates were obtained. Followed by adjusting the pH to 9 for an entire precipitation, the orange slurry was filtered and dry. The dried samples were separated into 7 parts and each part was dispersed into 60 mL of NaOH solution with a concentration of 0, 2, 4, 6, 8, 10 and 12 mol L^{-1}, respectively. Subsequently the slurry was transferred into 100 ml Teflon-lined autoclaves and heat to 473 K in an oven. After being crystallized for 24h, the products were washed with distilled water and dried at 80 °C for 4 h to remove possible residues, $Bi_2Fe_4O_9$ nanocrystals were finally obtained.

2.2 Characterizations

The phase composition of the $Bi_2Fe_4O_9$ nanocrystals was characterized by XRD (Bruker D8 Advance) with Cu Ka radiation. The morphology of the $Bi_2Fe_4O_9$ nanocrystals was investigated on a Hitachi S4800 SEM microscope. TEM and electron diffraction observations were carried out on a JEOL JEM2100F transmission electron microscope operated at 200 kV. UV-vis diffuse reflectance spectra were measured on a UV-vis spectrophotometer (Shimadzu UV2450).

2.3 Photoelectrochemical Measurements

The photocurrent density of the $Bi_2Fe_4O_9$ nanocrystals was measured in photoelectrochemical cell, which consists of three parts: a standard electrochemical workstation (CHI 760 C), a light source provided with a 300W Xe-arc lamp with/without a UV cutoff filter (≥420 nm), and a three-electrode photoelectrochemical cell with a working electrode, a reference electrode (Ag/AgCl) and a platinum counter electrode. All the photoelectrochemical measurements were carried out with a zero bias (vs. Ag/AgCl) in Na_2SO_4 electrolyte of 0.5 M without pH control which was exposed to air. The illumination area of each working electrode was 2.25 cm^2.

3 Results and Discussions

Fig. 1 shows the X-ray diffraction (XRD) patterns of the filtered and dried precipitation after adjusting the pH of mix solution to 9 and products after the hydrothermal treatment. It can be found that the precipitation shows an amorphous phase, judging from the broad peak at about 30° in the XRD pattern. The crystallization of the precipitation can be observed after the hydrothermal treatment at various NaOH added. It is clearly that the main phase of the samples were mullite-type $Bi_2Fe_4O_9$ (JCPDS No. 25-0090) when prepared under hydrothermal treatment microenviroment of NaOH concentration higher than 6.0 mol L^{-1}, demonstrating that single-phase $Bi_2Fe_4O_9$ crystals were obtained. However, when the concentration of NaOH is lower, mix phases ferrite compounds are formed.

4 The Morphologies of $BiVO_4$

Figure 2 shows the typical scanning electron microscopy (SEM) micrograph of the nanocrystals synthesized by co-precipitation of aqueous ammonia solution, followed by hydrothermal treatment at various microenviroments. It showed different particle shapes of $Bi_2Fe_4O_9$ had been formed. At the presence of a higher concentration of NaOH, the particle-size of $Bi_2Fe_4O_9$ became a platelet shape. However, a further increasing of the NaOH concentration, the surface of $Bi_2Fe_4O_9$ became corrode, suggesting that high concentration of NaOH results in the surface destroyment of $Bi_2Fe_4O_9$ nanocrystals. It is thus concluded that the processes occurring in the microenviroment is vital for the morphology of the samples.

Fig. 3 shows the ultraviolet-visible (UV-vis) absorption spectrum of the $Bi_2Fe_4O_9$ nanocrystals transformed from the diffuse reflection spectrum according to the Kubelka–Munk theory. It can be seen that the $Bi_2Fe_4O_9$ nanocrystals have absorptions from UV to visible light and two absorption edges are present at about 500 nm and 700 nm, respectively. It has been reported that $Bi_2Fe_4O_9$ is a multiband semiconductor.[13] Its conduction band bottom (E_c) and middle narrow bands (E_m) mainly consist of split Fe 3d orbitals, while the valence band top (E_v) mainly consists of O_{2p} orbitals. The two absorption edges are ascribed to split Fe 3d transitions. The two insets of Fig. 4 display the plots of $(Ahv)^2$ versus photon energy h around the absorption edges. According to the classical Tauc approach,[23] the two bandgaps of $Bi_2Fe_4O_9$ nanocrystals are calculated to be 2.05 eV and 1.57 eV, respectively. The two narrow bandgaps indicate that $Bi_2Fe_4O_9$ is good at absorbing solar light, especially visible light.

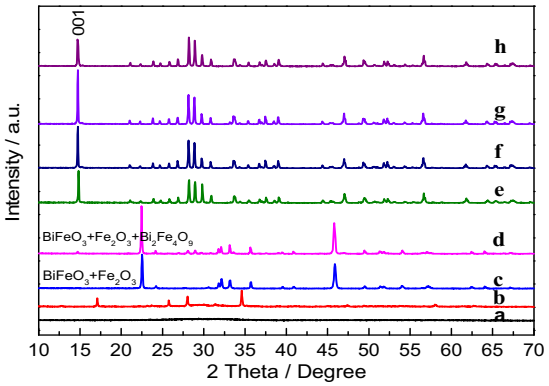

Fig.1 XRD patterns of (a) precipitation after added NH3.H2O and Bi2Fe4O9 crystals hydrothermally synthesized under the presence of (b) 0 M NaOH; (c) 2 M NaOH; (d) 4 M NaOH; (e) 6 M NaOH; (f) 8 M NaOH; (g) 10 M NaOH; (h) 12 M NaOH.

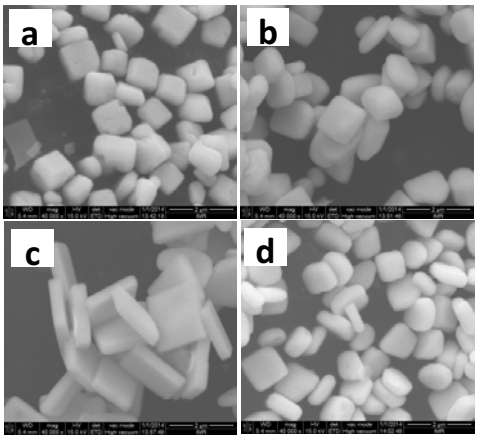

Fig.2 SEM patterns of $Bi_2Fe_4O_9$ crystals hydrothermally synthesized under the presence of (a) 6 M NaOH; (b) 8 M NaOH; (c) 10 M NaOH; (d) 12 M

Fig. 4 shows the time dependences of photocurrent for the $Bi_2Fe_4O_9$ nanocrystals upon chopped visible-light and full-light irradiations, respectively. Prompt and steady photocurrent density of 39 mA cm^{-2} was observed in the $Bi_2Fe_4O_9$ nanocrystals thin-film hydrothermally synthesized under the presence of 8 M NaOH under visible light, while 35 $mA.cm^{-2}$ photocurrent was obtained for the thin-film in the presence of 6 M NaOH. The good stability of photocurrent indicates that an efficient charge transfer took place in the thin-film photoelectrode made of the $Bi_2Fe_4O_9$ nanocrystals. Intrinsically, the energy band structure of the $Bi_2Fe_4O_9$ nanocrystals is very suitable for solar absorption to generate electron–hole pairs. On the other hand, the activity of different crystal facets can affect the solar absorption performance. Among the (001), ($\bar{1}$10) and (110) facets of $Bi_2Fe_4O_9$, UV irradiation can activate all the three facets, while visible-light irradiation only activates ($\bar{1}$10) and (110) facets of high-surface energy.[19] In our $Bi_2Fe_4O_9$ nanocrystals, both the predominant nanorods and nanocubes exhibit high percentage of exposed (110)/($\bar{1}$10) facets and thus high reactivity to absorb solar light, especially visible light. Therefore, they are more effective in utilizing

solar energy to generate electron–hole pairs. In addition, the nanoscale size of $Bi_2Fe_4O_9$ facilitates the separation of the excited electrons and holes before their loss via recombination to improve the photo-to-current efficiency.

In summary, pure-phase $Bi_2Fe_4O_9$ nanocrystals were successfully prepared via a simple and controllable chemical co-precipitation method. The nanocrystals consist of nanorods grown along (001) and nanoparticles. Their dominating facets are (001), (110) and ($\bar{1}$10). The nanorods were formed through oriented attachment of nearly cube-shaped nanoparticles. The nanocrystals exhibit two narrow bandgaps of 2.05 eV and 1.57 eV, indicating that the nanocrystals are good at absorbing solar light, especially visible light. Steady photocurrent as high as 39 mA cm^{-2} was observed in the $Bi_2Fe_4O_9$ nanocrystals under visible-light irradiation. These results suggest that the $Bi_2Fe_4O_9$ nanocrystals are promising for applications in photoelectrode and solar energy conversion.

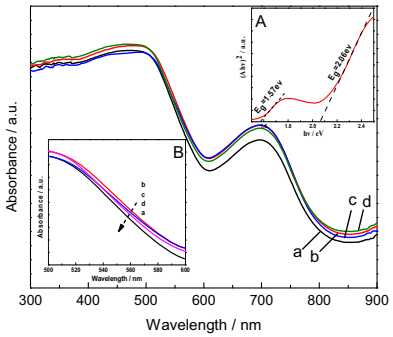

Fig.3 Difuse-reflectance spectroscopy $Bi_2Fe_4O_9$ crystals hydrothermally synthesized under the presence of (a) 6 M NaOH; (b) 8 M NaOH; (c) 10 M NaOH; (d) 12 M NaOH.

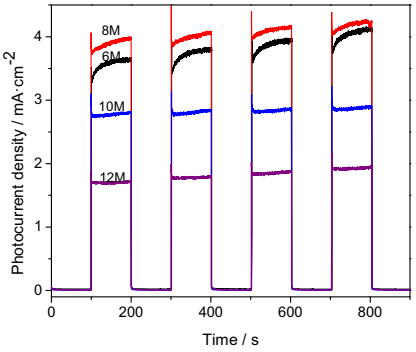

Fig.4 The photocurrent density of $Bi_2Fe_4O_9$ thin-film hydrothermally synthesized under the presence of (a) 6 M NaOH; (b) 8 M NaOH; (c) 10 M NaOH; (d) 12 M NaOH.

Acknowledgements

This work was financially supported by the China Postdoctoral Science Foundation (2014M551869), Shandong Excellent Young Scientist Research Award Fund (BS2015CL002), and Qingdao Postdoctoral Application Research Fund.

References

1. G. Catalan and James F. Scott, Physics and Applications of Bismuth Ferrite, Adv. Mater. 21 (2009) 2463–2485.
2. M. Liu, C. Lin, Y. L. Gu, T.Y. Yang, Z. L. Gong, G. Z. Yin, X.Y. Gao, X. T. Zhou, W. Wen, *J. Phys. Chem. C* 118 (2014) 14711-14722.
3. A.S. Poghossian, H.V. Abovian, P.B. Avakian, S.H. Mkrtchian, V.M. Haroutunian, *Sensor Actuat. B: Chem.* 4 (1991) 545-549.

4. T. Devendra, F. David J., Chaudhuri, T. K., Solution Processed Bismuth Ferrite Thin Films for All-Oxide Solar Photovoltaics, *J. Phys. Chem. C* 119 (2015) 5872-5877.
5. X.Y. Zhang, J. Lv, L. Bourgeois, J.W. Cui, Y.C. Wu, H. T. Wang, P. A. Webley, Formation and photocatalytic properties of bismuth ferrite submicrocrystals with tunable morphologies *New J. Chem.* 35 (2011) 937-941.
6. S.M. Sun, W.Z. Wang, L. Zhang, M. Shang, Visible Light-Induced Photocatalytic Oxidation of Phenol and Aqueous Ammonia in Flowerlike $Bi_2Fe_4O_9$ Suspensions *J. Phys. Chem. C* 113 (2009) 12826-12831.